doi:10.1111/evo.13315

Mechanical and tactile incompatibilities cause reproductive isolation between two young damselfly species

Alexandra A. Barnard,[1,2] Ola M. Fincke,[1] Mark A. McPeek,[3] and John P. Masly[1]

[1] *Ecology & Evolutionary Biology Program, Department of Biology, University of Oklahoma, Norman, Oklahoma*

[2] *E-mail: alex.barnard@ou.edu*

[3] *Department of Biological Sciences, Dartmouth College, Hanover, New Hampshire*

Received May 27, 2017
Accepted July 11, 2017

External male reproductive structures have received considerable attention as a cause of reproductive isolation (RI), because the morphology of these structures often evolves rapidly between populations. This rapid evolution presents the potential for mechanical incompatibilities with heterospecific female structures during mating and could thus prevent interbreeding between nascent species. Although such mechanical incompatibilities have received little empirical support as a common cause of RI, the potential for mismatch of reproductive structures to cause RI due to incompatible species-specific tactile cues has not been tested. We tested the importance of mechanical and tactile incompatibilities in RI between *Enallagma anna* and *E. carunculatum*, two damselfly species that diverged within the past ~250,000 years and currently hybridize in a sympatric region. We quantified 19 prezygotic and postzygotic RI barriers using both naturally occurring and laboratory-reared damselflies. We found incomplete mechanical isolation between the two pure species and between hybrid males and pure species females. Interestingly, in mating pairs for which mechanical isolation was incomplete, females showed greater resistance and refusal to mate with hybrid or heterospecific males compared to conspecific males. This observation suggests that tactile incompatibilities involving male reproductive structures can influence female mating decisions and form a strong barrier to gene flow in early stages of speciation.

KEY WORDS: Genitalia, Odonata, reproductive isolation, speciation.

Understanding speciation requires identifying how reproductive isolation (RI) is initiated and maintained in the early stages of population divergence (Coyne and Orr 2004; Butlin et al. 2012). Over the past century, speciation researchers have used a variety of experimental and comparative approaches to identify which barriers appear most important in causing RI early in the speciation process. These efforts have revealed that sexual isolation and ecological divergence tend to evolve earlier than hybrid sterility and inviability in both plants (e.g., Grant 1992; Ramsey et al. 2003; Husband and Sabara 2004; Kay 2006) and in animals (e.g., McMillan et al. 1997; Price and Bouvier 2002; Mendelson and Wallis 2003; Dopman et al. 2010; Sánchez-Guillén et al. 2012; Williams and Mendelson 2014; Castillo et al. 2015). Prezygotic isolation also typically evolves faster in sympatry than in allopatry, and hybrid sterility typically evolves faster than hybrid inviability (Coyne and Orr 1997; Presgraves 2002; Price and Bouvier 2002; Russell 2003). Identifying the traits that diverge to cause RI underlying these broad patterns is a major goal of speciation research.

One set of traits that has received much attention because of their rapid rates of evolutionary change is external reproductive structures. In internally fertilizing animals, male intromittent genitalia are among the fastest evolving external morphological traits, and genital morphological variation can affect reproductive fitness within species (Eberhard 1985; Otronen 1998; Danielsson and Askenmo 1999; House and Simmons 2003; Rodriguez et al. 2004; Bertin and Fairbairn 2005; Simmons et al. 2009). Likewise, nonintromittent contact or grasping structures often show similar patterns of rapid, divergent evolution, and divergence in these structures can also affect reproductive success within species

This article corresponds to Isaacson, J. (2017). Digest: Premating barriers drive reproductive isolation between two damselfly species. Evolution. https://doi.org/10.1111/evo.13331.

(Arnqvist 1989; Bergsten et al. 2001; Wojcieszek and Simmons 2012).

Rapid divergence of reproductive structures between populations has been hypothesized to cause RI via two different mechanisms. The first is mechanical incompatibility (Dufour 1844), in which structural incompatibilities between male and female genitalia of different species prevent successful copulation and reproduction. Mechanical incompatibilities have been documented in some animal species pairs (Jordan 1896; Standfuss 1896; Federley 1932; Schick 1965; Paulson 1974; Sota and Kubota 1998; Tanabe and Sota 2008; Kamimura and Mitsumoto 2012; Sánchez-Guillén et al. 2012; Wojcieszek and Simmons 2013; Sánchez-Guillén et al. 2014; Anderson and Langerhans 2015), although this mechanism of RI has not received broad support as a common mechanism of RI between young species (Shapiro and Porter 1989; Masly 2012; Simmons 2014).

The second proposed mechanism is tactile incompatibility (de Wilde 1964; Eberhard 1992), in which mismatch between male and female genitalia of different species prevents or reduces the success of mating and reproduction because one or both sexes fail to stimulate the other in the proper species-specific manner. The essence of this idea is that female reproductive decisions are based on the pattern of tactile stimuli transmitted by the male, and improper stimulation can result in female refusal to mate, early termination of mating, or lowered postcopulatory fitness, including reduced reproductive fitness in hybrid offspring (Eberhard 2010). Tactile isolation likely operates in a similar manner as other sensory modalities involved in mate choice and species recognition such as auditory or chemical signals, in which quantitative variation exists in male traits and female preferences (Ryan and Wilczynski 1991; Shaw 1996; Tregenza and Wedell 1997; Singer 1998; Johansson and Jones 2007). If females discriminate among the mating structures of conspecific mates, female discrimination against heterospecific males can arise as a byproduct of sexual selection within species (reviewed in Panhuis et al. 2001; Turelli et al. 2001; Simmons 2014). Thus, any mismatch between male morphology and female response to stimulation from a particular morphology could result in reduced reproductive success when females mate with a heterospecific male or an interspecific hybrid male. The importance of tactile incompatibilities remains unknown, although there is good reason to expect that these incompatibilities may occur frequently (Simmons 2014), and therefore have the potential to play a significant role in the evolution of RI.

Because identifying the effects of tactile incompatibilities requires carefully quantifying mating behavior and physiology, these incompatibilities have often been overlooked in tests of RI involving divergence of reproductive structures (Masly 2012). Nonetheless, some evidence for tactile incompatibility in the absence of mechanical incompatibilities exists in butterflies (Lorkovic 1953, 1958), scarab beetles (Eberhard 1992), *Drosophila* (Coyne 1993; Price et al. 2001; Frazee and Masly 2015—but see LeVasseur-Viens et al. 2015), and sepsid flies (Eberhard 2001). Notably, damselflies (Odonata, suborder Zygoptera) are often touted as a prime example of the importance of both mechanical and tactile incompatibilities in RI among closely related species. The potential for either mechanism to cause RI has been particularly well described in the families Lestidae and Coenagrionidae, whose males do not engage in premating courtship or visual displays (Williamson 1906; Krieger and Krieger-Loibl 1958; Loibl 1958; Paulson 1974; Tennessen 1975; Robertson and Paterson 1982; Hilton 1983; Battin 1993; Sánchez-Guillén et al. 2012; Sánchez-Guillén et al. 2014). Male damselflies have two sets of paired grasping organs at the end of their abdomen (Fig. 1). A male initiates the mating sequence by grasping the female's thorax with these appendages to form the "tandem" position. The species-specific male appendages and female thoracic structures engage such that structural mismatch appears to prevent many heterospecific tandems from forming (Paulson 1974). Mechanical isolation appears to be a major cause of RI in *Ischnura* (Krieger and Krieger-Loibl 1958; Sánchez-Guillén et al. 2014). For *Ischnura* species pairs with incomplete mechanical isolation, tactile isolation has been suggested to contribute to RI (Sánchez-Guillén et al. 2012; Wellenreuther and Sánchez-Guillén 2016), although this idea has not been tested quantitatively.

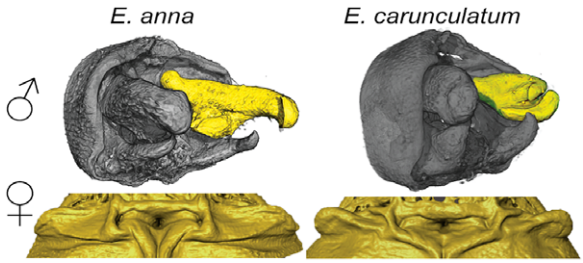

Figure 1. Male grasping appendages and female mesostigmal plate morphology. The right cercus on each male is shaded yellow.

Mechanical isolation also appears to prevent many heterospecific tandems in *Enallagma*, the most speciose North American genus (Paulson 1974; Miller and Fincke 2004; Fincke et al. 2007). Divergence in reproductive structure morphology is associated with a relatively recent *Enallagma* radiation (250,000-15,000 years ago; McPeek et al. 2008). Importantly, the rapid morphological diversification was not accompanied by marked ecological divergence among many *Enallagma* species (Siepielski et al. 2010). Although male cerci (superior terminal appendages) and female thoracic plates show a pattern of correlated evolution within *Enallagma* species (McPeek et al. 2009), species-specific divergence in these structures does not always cause strong mechanical incompatibilities, and interspecific tandems are occasionally observed

(Paulson 1974; Tennessen 1975; Bick and Bick 1981; Forbes 1991; Miller and Fincke 2004; Fincke et al. 2007). After tandem formation, female *Enallagma* control whether copulation occurs and they typically refuse to mate with heterospecifics or males whose cercus morphology has been manipulated (Robertson and Paterson 1982). *Enallagma* mesostigmal plates contain mechanoreceptors in species-specific locations that appear to be contacted by the male cerci during tandem, which may allow female assessment of a male's cercus morphology (Robertson and Paterson 1982).

Although prezygotic isolating barriers appear to evolve earlier than postzygotic barriers in damselflies (Sánchez-Guillén et al. 2012; Sánchez-Guillén et al. 2014), the relative importance of mechanical and sensory mechanisms of prezygotic RI remains unclear for two reasons. First, it can be difficult to distinguish between mechanical and tactile mechanisms experimentally: if a male-female pair fails to form a tandem, it is often unclear whether the incompatibility is purely mechanical or whether it involves tactile or behavioral cues that cause one sex to reject the other (Tennessen 1975; Robertson and Paterson 1982; Shapiro and Porter 1989). Second, mechanical isolation or male–female "fit" is not always defined in a way that makes quantifying variation in these phenotypes straightforward (Masly 2012). This lack of clarity over what constitutes mechanical incompatibility has led to conflation of mechanical RI (i.e., failure of male and female parts to engage) in damselflies with mechanisms that might be better described as tactile (Tennessen 1982).

Distinguishing mechanical from tactile mechanisms requires performing detailed mating observations among males and females that possess interspecific variation in reproductive structures and identifying specific features of reproductive morphology that prevent mating or reduce mating success using high-resolution phenotypic data. Here, we take advantage of a large collection of naturally occurring interspecific hybrids and laboratory-generated hybrids to test the hypothesis that divergence in reproductive structural morphology causes RI at the early stages of speciation in damselflies. We measure 19 potential pre- and postzygotic isolating barriers between *Enallagma anna* and *E. carunculatum*, two species that diverged from a common ancestor sometime in the last ~250,000 generations (McPeek et al. 2008; Callahan and McPeek 2016) and co-occur over much of the western United States (Westfall and May 2006). Both species have identical ecologies and overall morphologies (Turgeon et al. 2005; McPeek et al. 2009), but display conspicuous differences in the size and shape of the male cerci and female mesostigmal plates (Fig. 1). We quantify variation in male and female reproductive structure morphologies, distinguish mechanical and tactile premating incompatibilities, estimate the cumulative strengths of multiple reproductive barriers, and independently test predictions of mechanical and tactile isolation hypotheses (Richards and Robson 1926; Shapiro and Porter 1989). If mechanical incompatibilities occur, male *E. anna* × *E. carunculatum* hybrids that possess intermediate cercus morphologies will have less success at forming tandems compared to conspecific males. If tactile incompatibilities occur, males will be able to achieve tandem regardless of their cercus morphology, but females will refuse to mate with males whose morphologies deviate significantly from the conspecific mean phenotype.

Materials and Methods

Damselfly cerci and mesostigmal plates are non-intromittent sexual structures that are not directly involved in the transfer of gametes from male to female. However, terminal appendages of male insects and the female structures they contact during mating are often referred to as secondary genital structures. We thus include them as genital traits, consistent with previous definitions (Eberhard 1985; Arnqvist and Rowe 2005; Eberhard 2010; Simmons 2014; Brennan 2016) and refer to them generally as "genitalia" in the presentation of our results.

NATURAL POPULATION SAMPLING

We studied wild populations of *E. anna* and *E. carunculatum* in July and August 2013 at a site on the Whitefish River (Montana, U.S.A.; 48°22′15″N 114°18′09″W), where putative interspecific hybrids have been reported (Miller and Ivie 1995; Westfall and May 2006). To estimate relative frequencies of each species, we collected solitary males and tandem/copulating male–female pairs during peak activity between 1030 and 1600 h. We initially assigned species identity after inspecting cercus and mesostigmal plate morphology with a hand lens or dissecting microscope, respectively. Males and females with morphologies that appeared intermediate were initially designated as hybrids. We reassessed these assignments in the laboratory after 3D morphometric analysis (see next). We calculated the proportions of *E. anna*, *E. carunculatum*, and hybrid males from all sampling bouts and used these male frequencies to estimate the expected frequencies of each type of male–female pair under random mating.

We attempted to cross virgin *E. anna* and *E. carunculatum* to measure postzygotic RI between pure species, but we did not obtain heterospecific copulations in either cross direction. Instead, we established laboratory populations of hybrids and parental species by collecting eggs from mated pairs captured in the field. Offspring of field-caught pairs are hereafter referred to as "laboratory generation 1." Mated females oviposited on moist filter paper, which was kept submerged in 2–4 cm of water until larvae hatched. We obtained embryos from 24 *E. anna* pure species crosses, 32 *E. carunculatum* pure species crosses, and eight mixed crosses: one *E. carunculatum* female × *E. anna* male, one *E. anna*

female × *E. carunculatum* male, one *E. carunculatum* female × hybrid male, and five hybrid female × *E. anna* male ("hybrid" refers to damselflies with intermediate cercus or mesostigmal plate morphologies). After sampling, egg collection, and behavioral observation, we stored adult damselflies in 95% ethanol for subsequent morphometric analyses.

LABORATORY REARING

We transported embryos from the field site to the University of Oklahoma Aquatic Research Facility where the larvae hatched and were reared to adulthood in individual 140 mL cups. These laboratory generation 1 larvae were provided with *Artemia*, *Daphnia*, or *Lumbriculus* as food sources and experienced a natural photoperiod and daily water temperatures that averaged 20.0 ± 0.19°C. We housed adults in mesh cages (30.5 cm^3; BioQuip, Rancho Dominguez, CA, USA), segregated by sex until sexual maturity and provided them with adult *Drosophila* as a food source ad libitum. We used laboratory generation 1 virgin adults to quantify prezygotic barriers, plus additional postzygotic barriers that we could not measure in the field. We mated 24 adult pairs from this first laboratory generation: 11 *E. anna*, two *E. anna* female × hybrid male, two *E. carunculatum* female × hybrid male, six hybrid female × *E. anna* male, and four hybrid female × hybrid male, and raised them under the conditions described above. Embryos from these crosses (hereafter, "laboratory generation 2") contributed fecundity, fertility, and hatch rate data but were not raised to adulthood due to difficulties with rearing them. Mated adults were stored in 95% ethanol after mating (males) or after oviposition (females). Unmated damselflies were maintained to calculate captive life span, then preserved in 95% ethanol.

MORPHOMETRIC ANALYSIS

We photographed ethanol-preserved adults using a Nikon D5100 camera (16.2 MP; Nikon Corporation, Tokyo, Japan) and measured abdomen length (abdominal segments one to 10, excluding terminal appendages) as a proxy for body size using ImageJ (Abramoff et al. 2004) for 175 males and 171 females. To reduce measurement error, we measured each abdomen twice, then used the mean length in subsequent analyses after confirming that repeatability was high for the separate measurements (r = 0.97). We obtained 3D digital reconstructions of male cerci and female mesostigmal plates by scanning 140 male terminal segments and 162 female thoraces in a SkyScan 1172 microcomputed tomography scanner (Bruker microCT, Kontich, Belgium). Male structures were scanned at a voxel resolution of 2.36 or 2.53 μm, and female thoraces at 2.78 or 3.88 μm, and the scan data were converted to image stacks using NRecon version 1.4.4 (Bruker microCT).

To quantify cercus shape, we digitally segmented the right cercus from each male's image stack and converted it to a solid surface object using Avizo Fire software (FEI Software; Hillsboro, OR, USA) as described in McPeek et al. (2008). We measured the volume of each cercus object as a proxy for cercus size, using Avizo's volume measurement tool. To quantify and compare their shapes, each cercus was represented by a mesh of 20,000 triangles with 10,002 vertices, each defined by distinct (x, y, z) coordinates (Fig. S1). We placed seven landmarks on common points on each cercus, then used these landmarks to register all digitized cerci in identical orientations within the coordinate plane. To ensure that only shape and not size was compared in the analysis, all objects were standardized to have the same centroid size. Next, we performed spherical harmonic analysis (Shen et al. 2009), which represents the shape of a closed surface in terms of the sum of 3D sines and cosines on a sphere. We performed the analysis using 18 degrees of spherical harmonic representation, which captures relevant surface detail without introducing excess noise (Shen et al. 2009). The analysis generated 1083 coefficients to describe the shape of each cercus, which we reduced into the primary axes of shape differentiation using principal component (PC) analysis.

Because female mesostigmal plates are relatively flat structures, we represented plate morphology using 3D geometric morphometrics. For each female plate, we assigned 11 fixed landmarks and 248 sliding semi-landmarks to the right anterior thorax of each female (Fig. S2) using Landmark software (Wiley et al. 2005). We imported landmark coordinates into R and used the Geomorph package (version 2.1.7; Adams and Otarola-Castillo 2013) to assign 79 landmarks as "curve sliders" on the medial thorax and around the plate periphery, and 169 "surface sliders" evenly spaced across the plate. We obtained 3D shape variables for these representations using general Procrustes analysis superimposition (Rohlf 1999), then obtained a smaller set of plate shape variables from the Procrustes-superimposed coordinates using PC analysis.

MEASURING PRE- AND POSTZYGOTIC REPRODUCTIVE ISOLATING BARRIERS

To measure the strength of RI barriers between *E. anna* and *E. carunculatum*, we quantified 19 potential pre- and postzygotic isolating mechanisms that act from the beginning of the mating sequence through an individual's life history. Table 1 summarizes these RI measures and describes the equations used to estimate the absolute strength of each (Sobel and Chen 2014). Although it is often preferable to quantify RI using only reciprocal F_1 hybrids, the rarity of heterospecific crosses and our small sample of F_1 individuals made this impractical for estimating the strength of postzygotic RI barriers. Thus, to measure postzygotic barriers, we pooled all hybrid damselflies, including presumed F_1s from both cross directions and offspring from field-caught hybrids for which the exact genotypes were unknown.

Table 1. Formulas and data for the individual strength of each reproductive isolating barrier measured, listed in the order in which they act during the mating sequence and subsequent life history of an individual.

		A♀ × C♂			C♀ × A♂		
Barrier	RI formula	H	C	RI	H	C	RI
Prezygotic							
Visual	$1-2\times\left(\frac{\text{No. of het. tandem attempts}}{\text{No. of het.}+\text{con. tandem attempts}}\right)$	0.500	0.463	−0.038	0.537	0.500	−0.035
Precopulatory mechanical	$1-2\times\left(\frac{\text{Prop. het. tandems}}{\text{Prop. het.}+\text{con. tandems}}\right)$	0.667	0.950	0.175	0.250	1.000	0.600
Tactile I (female resistance)	$1-2\times\left(\frac{\text{Prop. het. tandems without resistance}}{\text{Prop. het.}+\text{con. tandems without resistance}}\right)$	0.333	0.923	0.469	0.286	0.800	0.474
Tactile II (female refusal)	$1-2\times\left(\frac{\text{Prop. het. matings}}{\text{Prop. het.}+\text{con. matings}}\right)$	0.143	0.447	0.516	0.125	0.833	0.739
Postzygotic							
Hybrid precopulatory mechanical	$1-2\times\left(\frac{\text{Prop. hyb. tandems}}{\text{Prop. hyb.}+\text{con. tandems}}\right)$	0.857	0.950	0.051	0.636	1.000	0.222
Hybrid tactile I (female resistance)	$1-2\times\left(\frac{\text{Prop. hyb. tandems without resistance}}{\text{Prop. hyb.}+\text{con. tandems without resistance}}\right)$	0.500	0.923	0.297	0.333	0.800	0.412
Hybrid tactile II (female refusal)	$1-2\times\left(\frac{\text{Prop. hyb. matings}}{\text{Prop. hyb.}+\text{con. matings}}\right)$	0.100	0.447	0.635	0.286	0.833	0.489
Hybrid copulatory mechanical	$1-2\times\left(\frac{\text{Prop. hyb. intromissions}}{\text{Prop. hyb.}+\text{con. intromissions}}\right)$	1.000	1.000	0.000	1.000	1.000	0.000
Copulation duration	$1-2\times\left(\frac{\text{Mean hyb. copulation duration}}{\text{Mean hyb.}+\text{con. copulation duration}}\right)$	21.900	19.900	−0.048	31.100	27.700	−0.058
Copulation interruption duration	$1-2\times\left(\frac{\frac{1}{\text{Mean duration, hyb. interruptions}}}{\frac{1}{\text{Mean duration, hyb.}}+\frac{1}{\text{Mean duration, con.}}}\right)$	0.444	0.971	0.372	nd	nd	nd

(*Continued*)

Table 1. Continued.

Barrier	RI formula	A♀ × C♂			C♀ × A♂		
		H	C	RI	H	C	RI
Oviposition	$1-2\times\left(\frac{\text{Prop. females oviposited, hyb. matings}}{\text{Females oviposited, hyb.} + \text{con. matings}}\right)$	0.769	0.943	0.101	1.000	0.941	−0.030
Fecundity	$1-2\times\left(\frac{\text{Mean no. of eggs laid, hyb. clutches}}{\text{Mean no. of eggs laid, hyb.} + \text{con. clutches}}\right)$	220.7	268.4	0.098	220.7	285.7	0.128
Fertility	$1-2\times\left(\frac{\text{Prop. fertilized eggs, hyb. clutches}}{\text{Prop. fertilized eggs, hyb.} + \text{con. clutches}}\right)$	0.870	0.900	0.017	nd	nd	nd
Egg hatching	$1-2\times\left(\frac{\text{Prop. hatched eggs, hyb. clutches}}{\text{Prop. hatched eggs, hyb.} + \text{con. clutches}}\right)$	0.987	0.928	−0.031	0.987	0.934	−0.028
Embryo development	$1-2\times\left(\frac{\text{Mean days oviposition to egg hatch, hyb.}}{\text{Mean days oviposition to egg hatch, hyb.} + \text{con.}}\right)$	19.400	18.600	−0.021	20.0	15.4	−0.130
Larval maturation	$1-2\times\left(\frac{\text{Mean days hatch to adult emergence, hyb.}}{\text{Mean days hatch to adult emergence, hyb.} + \text{con.}}\right)$	229.5	269.9	0.081	229.5	211.0	−0.042
Larval survivorship	$1-2\times\left(\frac{\text{Prop. hyb. larvae to reach adulthood}}{\text{Prop. hyb.} + \text{prop. con. to reach adulthood}}\right)$	0.060	0.057	−0.025	0.060	0.035	−0.265
Adult sex ratio	$1-2\times\left(\frac{\text{Prop. males, hyb. clutches}}{\text{Prop. males, hyb. clutches} + \text{prop. males, con. clutches}}\right)$	0.520	0.510	−0.010	0.520	0.500	−0.020
Total isolation				0.9937			0.9936

Prezygotic barriers refer to interactions between pure species and postzygotic barriers compare hybrid fitness (F_1s and advanced generations) to pure species.
con. = conspecific; het. = heterospecific; hyb. = hybrid; prop. = proportion; nd = no data.

Mate discrimination

We measured males' visual discrimination of potential mates by restraining individual field-caught *E. anna* and *E. carunculatum* females on wooden dowels near the water at the Whitefish River site and measuring the frequencies of each type of male that attempted tandem with them. We attached live females of each species by their legs to wooden dowels using Duco cement (ITW Devcon, Glenview, IL, USA; Miller and Fincke 1999) and placed individual dowels level with surrounding vegetation within 5 m of the water's edge. Over 20-min intervals, we captured each male that either attempted or achieved tandem with a restrained female and assigned them to species by examining the cerci with a hand lens. Males were held in paper envelopes until the end of the observation period to prevent the possibility of a second encounter with the restrained female and were then released.

Mating assays

We measured several premating RI barriers using mating experiments in which females were placed in mesh cages with either heterospecific, hybrid, or conspecific males. We used both field-caught and laboratory-reared damselflies, and used only virgin females in each mating assay. To obtain virgins in the field, we captured newly emerged females, identified by their pale teneral coloration. We assigned species identity as described above, then housed virgin females in cages until they reached sexual maturity (~10 days postemergence). We placed two to five individuals of each sex in a cage under partial shade in the grass and observed behaviors between 1000 and 1600 h.

We quantified precopulatory mechanical RI by measuring the frequency of tandem attempts in which the male was unable to securely grasp a female for longer than 5 sec. A secure hold was confirmed by observing the male flying while engaged with the female, or attempting to fly without losing contact while the female remained perched. We measured copulatory mechanical RI as the proportion of copulation attempts in which the male and female failed to achieve genital coupling. This estimates mechanical incompatibility between male grasping appendages and female thoracic plates and excludes the possibility of male loss of interest, because males were often observed repeatedly attempting tandem on the same female despite being unable to grasp her.

We quantified two types of precopulatory tactile incompatibilities using pairs that formed tandems. First, we recorded whether each female showed resistance behaviors during tandem (e.g., head shaking, wing flapping, dorsal abdominal extension, or body repositioning) (Tennessen 1975; Xu and Fincke 2011). Second, we recorded whether females in tandem cooperated in copulation or refused to mate.

Postzygotic isolation

We quantified several postmating RI barriers using both laboratory generations. We measured oviposition success as the proportion of females from each cross type that oviposited. When females failed to oviposit within three days postmating, we checked their male partners for motile sperm by anesthetizing them with CO_2, immediately dissecting out the seminal vesicle, gently squashing it under a coverslip, and examining the contents under a Zeiss Axio Imager 2 stereomicroscope (100 × total magnification). We dissected females that failed to oviposit to check the oviduct for mature eggs and the bursa copulatrix for sperm.

We calculated fecundity by counting all eggs laid by each mated female within three days of mating. The date of egg hatch was recorded as the first day that larvae were observed. We calculated the proportion of eggs that hatched from each clutch by counting the number of unhatched eggs that remained in the filter paper seven days after first hatch. We calculated fertility of laboratory-reared matings by counting the number of fertilized eggs, as indicated by a dark spot that develops on the apical end of the egg (Corbet 1999). We calculated embryo development time as days from oviposition to egg hatch, larval maturation as days from egg hatch to adult emergence, larval survivorship as the proportion of hatched larvae that emerged as adults, and adult sex ratio and total adult life span.

Strength of RI barriers

We estimated the absolute strength of each individual RI barrier using the following general equation (Sobel and Chen 2014):

$$\mathrm{RI} = 1 - 2 \times \left(\frac{H}{H + C}\right),$$

where H and C denote the frequency of heterospecific and conspecific interactions, respectively (prezygotic barriers), or fitness of hybrid or conspecific matings or offspring, respectively (postzygotic barriers; Table 1). This equation yields values between –1 and 1 in which 0 indicates no barrier to gene flow, 1 indicates complete RI, and –1 indicates complete hybrid advantage. In essence, the term $\frac{H}{H+C}$ describes the probability of gene flow between species. Larger values of the parameters H and C are typically associated with higher fitness in this equation. However, for duration of copulation interruptions, a larger value represents lower fitness. We therefore modified this equation by using the inverse of H and C values when calculating the contribution of copulation interruptions to RI. We estimated total RI between *E. anna* and *E. carunculatum* as described in Sobel and Chen (2014) for sympatric populations as:

$$\mathrm{RI}_{\mathrm{total}} = 1 - 2 \times \left(\frac{\prod_{i=1}^{n} P(H)_i}{\prod_{i=1}^{n} P(H)_i + \prod_{i=1}^{n} P(C)_i}\right).$$

We also used this same general equation to calculate cumulative RI for each barrier in the sequence, which yields each barrier's absolute contribution (*AC*). Finally, we used both of these values to calculate each barrier's relative contribution (*RC*) to total RI ($AC_i/\mathrm{RI}_{\mathrm{total}}$).

STATISTICAL ANALYSES

We compared males' sexual approaches toward con- and heterospecific females, observed versus expected frequency of heterospecific pairs, and adult sex ratios using binomial tests. We compared presence or absence of female resistance behaviors, female mating refusal or cooperation, frequency of copulation interruptions, and oviposition success among parental species and hybrid pairs using Fisher's exact tests. We examined the relationship between male abdomen length and cercus size using linear regression. We compared copulation and copulation interruption durations between conspecific and nonconspecific matings using *t* tests. We compared abdomen length, fecundity, fertility, proportion eggs hatched, developmental timing, and adult life span among *E. anna*, *E. carunculatum*, and hybrids using analysis of variance (ANOVA) after arcsin transformation of proportion data. When an ANOVA indicated a significant difference existed among the three groups for any measure, we conducted Tukey's post hoc tests to identify the differences among groups. For both forms of premating tactile isolation data, we omitted all cross types with sample size < 6 from statistical analyses. When possible, we combined data (field and laboratory, or laboratory generations 1 and 2) to increase statistical power, after confirming with ANOVA that measurements did not differ significantly between the two groups. All analyses were conducted in R version 3.1.1 (R Core Team 2015). Means are reported as ± 1 SEM.

Results and Discussion

MALES MATE INDISCRIMINATELY AND HYBRIDIZATION OCCURS AT LOW FREQUENCY IN NATURE

At the Whitefish River site, *E. anna* males outnumbered *E. carunculatum* males by a factor of ~1.5. This was observed for both solitary males (*E. anna*: $n = 165$, *E. carunculatum*: $n = 108$, over eight sampling days) and male–female pairs (*E. anna*: $n = 44$, *E. carunculatum*: $n = 28$, over nine sampling days). *E. anna* males attempted tandem with *E. carunculatum* females (46.3%, 19 of 41) as frequently as they did with *E. anna* females (53.7%, 22 of 41; $\mathcal{X}_1^2 = 0.010$, $P = 0.76$; Fig. 2). *Enallagma carunculatum* males also attempted tandem with females of both species equally (50.0%, eight of 16 each; $\mathcal{X}_1^2 = 0.00$, $P = 1.0$; Fig. 2). These results show that premating interactions between *E. anna* and *E. carunculatum* are random, similar to observations from other *Enallagma* (Paulson 1974; Fincke et al. 2007; Xu and Fincke 2011) and *Ischnura* species (Sánchez-Guillén et al. 2012; Sánchez-Guillén et al. 2014).

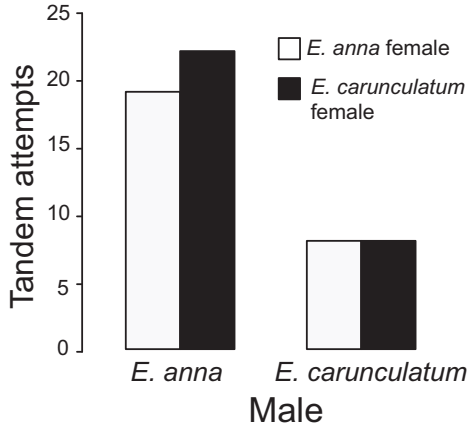

Figure 2. Male visual isolation. Number of male tandem attempts on conspecific and heterospecific females at the Whitefish River site.

Despite this lack of habitat and visual isolation in sympatry, heterospecific pairs were rarely captured in the field. In more than one month at the field site, we captured only two heterospecific male–female pairs, one in each cross direction. Based on the relative frequencies of each pure species, heterospecific pairs occur significantly less often than expected under random mating between *E. anna* and *E. carunculatum* ($\mathcal{X}_3^2 = 65.40$, $P < 1 \times 10^{-5}$). This suggests that although males may frequently initiate tandems with heterospecific females, such pairs likely remain in tandem only briefly. However, even the rare occurrence of both types of heterospecific tandems suggests that pure species may interbreed at low frequencies in the wild, and our collection of field-caught individuals supports this notion: 41 of 630 males and seven of 547 females we collected possessed intermediate reproductive structure morphologies that were visibly different from either pure species.

HYBRIDS ARE MORPHOLOGICALLY DISTINCT FROM EITHER PARENTAL SPECIES

Among males, the first five PC scores explained more than 77% of the cercus shape variance. PC1 (60.05%) distinguished pure species and represented differences in overall cercus length, from short (*E. carunculatum*) to long (*E. anna*), with hybrids showing a range of intermediate scores (Fig. 3A). PC2 (7.50%) represented a difference in the relative angles of the upper and lower projections of the cercus, with many hybrids occupying a different space along this axis than parental species. Most field-caught males we identified as hybrids had distinctly intermediate cercus morphologies, whereas the laboratory-reared males from heterospecific or backcross pairs possessed morphologies that spanned the entire

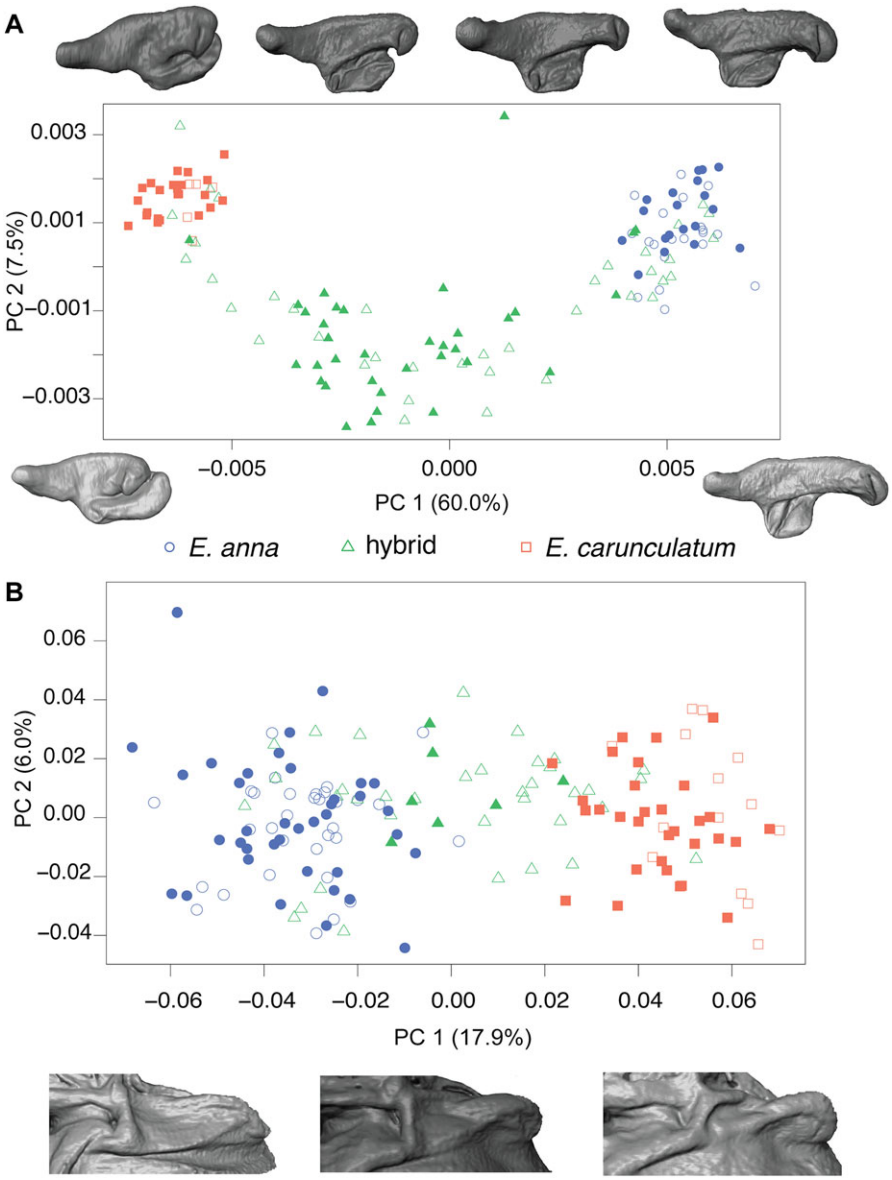

Figure 3. Variation in *E. anna*, *E. carunculatum*, and hybrid male and female reproductive structure morphologies. (A) Distribution of the first two principal components (PCs) that represent variation in male cercus shape. Cercus representations above the plot show the range of hybrid male variation across the PC1 axis and representations below the plot show parental species morphologies. (B) Distribution of the first two PCs that represent variation in female mesostigmal plate shape. Examples of representative parental species and hybrid morphologies are shown below the plot (left: *E. anna*, middle: hybrid, right: *E. carunculatum*). The percentage of variation explained by each PC axis is shown in parentheses. Open symbols represent laboratory-reared individuals, filled symbols represent field-caught individuals.

range of variation between *E. anna* and *E. carunculatum* males (Fig. 3A).

Among females, the first six PCs scores accounted for more than 42% of the variance in mesostigmal plate shape. *E. anna* and *E. carunculatum* specimens formed separate clusters along PC1 (17.9%), but there was considerable overlap between hybrids and *E. anna* on PC1 (Fig. 3B). This overlap might reflect limitations of the resolving power of our morphometric approach to distinguish intraspecific variation from intermediate hybrid morphology of these complex female structures. Additional PC axes indicated that parental species and hybrid plate shapes showed similar levels of variation in several features, including the angle of the plate's anterior edge relative to the thorax (PC2; 6.0%), curvatures of the plate's lateral edge (PC3; 5.5%) and plate surface (PC5; 4.6%), and dimensions of the space between the bilateral plates (PC4; 5.3%). Because slight variation in the manual placement of the fixed landmarks on each female has the potential to contribute to this apparent overlap between *E. anna* and the hybrid

females, we repeated the entire analysis beginning with placement of landmarks on a subset of 157 plates selected at random. Repeatability was high among landmark coordinates in both sets ($r > 0.99$) and both replicate analyses produced similar results (Fig. S3).

Our behavioral, rearing, and morphometric data confirm that individuals with intermediate reproductive structure morphologies are hybrids between *E. anna* and *E. carunculatum* and not a separate species as originally suggested (Miller and Ivie 1995). Interestingly, the collection of laboratory-reared hybrids (both F_1 and backcross) included cercus and plate phenotypes not observed in the field-caught samples (Fig. 3). Some laboratory-reared hybrid morphologies were even indistinguishable from those of the parental species, which could be the result of collecting eggs in the field from mated females that may have been storing sperm from previous conspecific matings. Alternatively, some field-caught adult damselflies that we designated as pure species may in fact have been hybrids that maintained "phenotypic integrity" with one parental species despite having highly admixed genomes (Poelstra et al. 2014). Despite this possibility of occasional misidentification, the majority of field-caught individuals we identified as hybrid possess morphologies that fall well outside of the distributions of either pure species. This is particularly true for cercus shape, which has pronounced differences between *E. anna* and *E. carunculatum*.

The distributions of the field-caught versus laboratory-reared hybrids also suggest that hybrid genital morphology may be under selection in the wild. In particular, the distribution of male morphologies shows that some laboratory-reared backcross hybrid males possess cercus morphologies rarely observed among field-caught males. This result suggests that although interspecific mating occurs in the field, F_1 hybrids either rarely backcross with parental species or backcross hybrids rarely survive to reproductive age. Our laboratory-rearing data show that hybrids can in fact backcross with parental species and advanced backcross individuals are viable and fertile (see next). However, future genomic studies will be needed to reveal the direction and genomic extent of introgression and the frequency of F_1 versus advanced-generation hybrids in the wild.

MECHANICAL INCOMPATIBILITIES CAUSE SUBSTANTIAL, ASYMMETRIC REPRODUCTIVE ISOLATION

Between pure species, precopulatory mechanical RI was incomplete in both directions of interspecific cross, and RI appears asymmetric: 25% (7/28) of *E. anna* males achieved tandems with *E. carunculatum* females, whereas 66.7% (6/9) of *E. carunculatum* males achieved tandems with *E. anna* females (Fig. 4A). These data show that mechanical isolation is relatively weak between *E. carunculatum* males and *E. anna* females, which presents

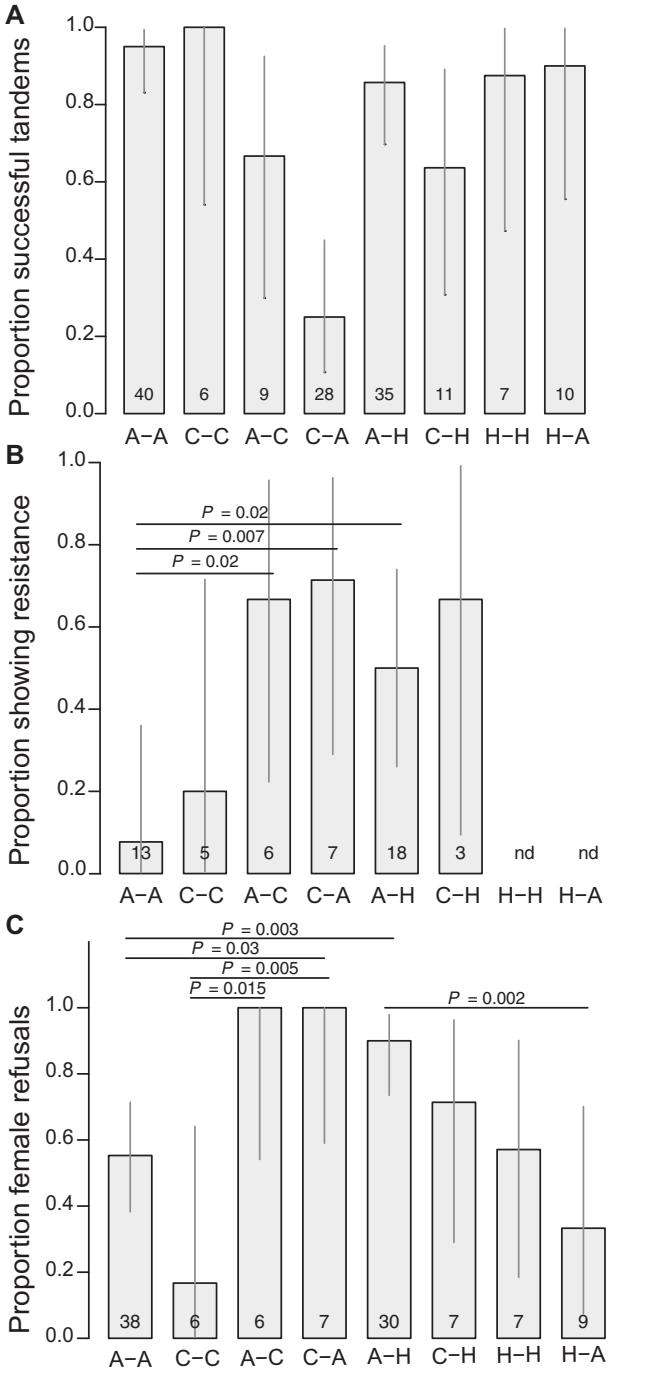

Figure 4. Sequentially acting mechanisms of prezygotic reproductive isolation. (A) Mechanical isolation. (B) Proportion of tandems in which females displayed resistance behaviors (field-caught only). (C) Proportion of tandems in which females refused to copulate (field-caught and laboratory-reared data). Crosses shown on the *x*-axis list female first. A: *E. anna*, C: *E. carunculatum*, H: hybrid. Numbers at the base of the bars in panels A-C show the numbers of female-male pairs that were measured. "nd" refers to cross types for which no data were collected. Error bars represent the upper and lower bounds of 95% binomial confidence intervals. For proportions of 0 or 1, bars represent one-sided 97.5% confidence intervals.

the opportunity for interspecific matings. Mechanical isolation due to males' inability to grasp heterospecific females is frequently evoked as the major contributor to RI in coenagrionid damselflies (Paulson 1974; Robertson and Paterson 1982; Fincke et al. 2007; Bourret et al. 2012; Wellenreuther and Sánchez-Guillén 2016), although several exceptions exist (Paulson 1974; Tennessen 1975; Bick and Bick 1981; Forbes 1991; Miller and Fincke 2004). Our results suggest that mechanical incompatibilities are not sufficiently strong enough to completely exclude the possibility of hybridization in *Enallagma*. Additionally, it has been suggested that species with longer cerci are better at grasping females of other species (Paulson 1974), but our data show that *E. anna* males, whose cerci are roughly twice as long as *E. carunculatum* cerci, were less capable of grasping heterospecific females compared to *E. carunculatum* males.

The existence of incomplete precopulatory mechanical incompatibilities between *E. anna* and *E. carunculatum* suggests that the intermediate cercus morphology of hybrid males might reduce their ability to form tandems with pure species females. Eighty-six percent (30/35) of hybrid males we tested achieved tandem with *E. anna* females, and 63.6% (7/11) achieved tandem with *E. carunculatum* females (Fig. 4A). Thus, male hybrids achieved tandem with both pure species more frequently than males of either pure species achieved tandem with heterospecific females. These results show that although hybrid males were less successful at forming tandems with females than conspecific males, they were more successful than heterospecific males.

Mechanical incompatibility involving the primary genitalia (intromittent organs) may also cause RI. No heterospecific matings occurred during our behavioral observations, so we could not directly measure copulatory mechanical RI between *E. anna* and *E. carunculatum*. However, among the tandem pairs involving hybrids in which the female initiated copulation (two *E. anna*, two *E. carunculatum*, and three hybrid females), all seven pairs achieved genital coupling. Although this sample size is modest, this result suggests that no copulatory mechanical incompatibility exists between hybrids and parental species. This is not unexpected, as *E. anna* and *E. carunculatum* penes have similar morphologies (Kennedy 1919). Taken together, the results from these mating assays show that as the morphological mismatch between interacting male and female mating structures increases, the possibility of forming tandem and mating decreases.

TACTILE INCOMPATIBILITIES CAUSE SUBSTANTIAL RI WHEN MECHANICAL ISOLATION IS INCOMPLETE

A significantly greater proportion of laboratory-reared *E. anna* females (12/22) engaged in resistance behaviors during conspecific tandems than did field-caught *E. anna* females (one of 13, Fisher's exact test, $P = 0.01$). For this reason, we analyzed presence/absence of female resistance during tandem separately for field-caught and laboratory-reared populations. In the field, *E. anna* females were significantly more likely to resist during tandems with heterospecific males (67%; four of six) or hybrid males (50%; nine of 18) than with conspecific males (7.7%; one of 13; Fisher's exact tests, $P_{\text{heterospecific}} = 0.02$, $P_{\text{hybrid}} = 0.02$; Fig. 4B). Additionally, 71.4% (five of seven) of *E. carunculatum* females displayed resistance behaviors during tandem with *E. anna* males in the field, which was significantly greater than 7.7% of *E. anna* females ($P = 0.007$; Fig. 4B).

Surprisingly, laboratory-reared *E. anna* females resisted during tandems with conspecific males as frequently as they resisted during tandems with hybrid males (54.5%, 12 of 22 vs. 81.8%, nine of 11, respectively; $P = 0.25$; Fig. S4). *Enallagma anna* and hybrid females also showed similar levels of resistance during tandem with *E. anna* males (14.3%, one of seven of hybrid females resisted; $P = 0.09$; Fig. S4). A comparison of the two reciprocal *E. anna* × hybrid crosses, however, showed that *E. anna* females were significantly more likely to resist during tandem with hybrid males (81.8%) than were hybrid females (14.3%; $P = 0.01$; Fig. S4). Female resistance during tandem with a conspecific male is not unusual (Tennessen 1975; Fincke 2015), but because the field-caught and laboratory-reared *E. anna* populations behaved so differently, and the field data reflects behavior in a natural setting, we used the field-caught female data to calculate this form of tactile isolation (Table 1).

Field-caught and laboratory-reared females showed similar copulatory refusal rates: 94.7% (18 of 19) field-caught and 81.8% (nine of 11) laboratory-reared *E. anna* females refused hybrid males (Fisher's exact test, $P = 0.54$), and 69.2% (nine of 13) field-caught and 51.9% (12/25) laboratory-reared *E. anna* females refused conspecific males ($P = 0.31$). We therefore pooled field-caught and laboratory-reared data to analyze female copulation refusal or acceptance. Ninety percent (27/30) of *E. anna* females taken in tandem by hybrid males refused to copulate, which was significantly greater than the 55.3% (21/38) of *E. anna* females that refused conspecific males ($P = 0.003$; Fig. 4C). All six *E. anna* females observed in tandem with *E. carunculatum* males refused to copulate, although this level of refusal was not statistically different from the conspecific refusal rate ($P = 0.07$; Fig. 4C). This is likely due to the low number of heterospecific pairs we could observe. *Enallagma carunculatum* females, in contrast, were significantly more likely to refuse an *E. anna* male (100%, all of the seven) than a conspecific male (16.7%, one of six; $P = 0.005$; Fig. 4C). *Enallagma anna* females also refused to mate with *E. carunculatum* males more frequently than did *E. carunculatum* females ($P = 0.015$). We obtained a similar result for the reciprocal cross, where more female *E. carunculatum* females refused *E. anna* males than did *E. anna* females ($P = 0.03$; Fig. 4C).

Females' behavioral responses to different types of males reveal strong assortative mating between *E. anna* and *E. carunculatum* when premating mechanical isolation fails. Tactile isolation also predicts that pure species females should refuse to mate with hybrid males because intermediate cerci fail to relay the proper tactile species recognition signal to the female. Our behavioral data support this prediction for *E. anna* females, which mated with hybrid males less frequently than with conspecific males. The finding that some *E. anna* females mated with hybrid males, but none mated with *E. carunculatum* males suggests that females display some latitude in their preferences and are more likely to refuse males whose cercus morphology greatly deviates from a conspecific phenotype. Although incomplete mechanical isolation has been documented in several *Enallagma* species pairs, few cases of hybridization are known, based on morphological or genetic evidence (Catling 2001; Turgeon et al. 2005; Donnelly 2008). This suggests that even with incomplete mechanical isolation, tactile isolation might prevent interbreeding among most *Enallagma* species. A full understanding of tactile isolation will require quantitative study of the mechanoreceptors on female plates to understand how patterns of phenotypic variation might contribute to RI.

The relative sizes of male and female reproductive structures may influence both mechanical and tactile mechanisms of RI. Larger males tended to have larger cerci, as indicated by regressing cercus volume on abdomen length (*E. anna*: $F_{1,26} = 18.80$, $R^2 = 0.397$, $P = 0.0002$; *E. carunculatum*: $F_{1,17} = 7.744$, $R^2 = 0.273$, $P = 0.013$). Hybrids, however, showed a weaker relationship between body size and cercus size, because hybrids display more variation in cercus morphology than either parental species ($F_{1,55} = 6.70$, $R^2 = 0.092$, $P = 0.01$). A size mismatch in male and female structures either within or between species may contribute to mechanical incompatibilities, although our current data do not allow us to examine that relationship robustly.

POSTMATING BARRIERS CONTRIBUTE LITTLE TO REPRODUCTIVE ISOLATION

Compared to the strong premating RI caused by mechanical and tactile incompatibilities of male and female reproductive structures, we found relatively weak RI from postmating barriers. Copulation duration was similar among conspecific mating pairs and pairs including at least one hybrid partner ($t_{25} = -0.028$, $P = 0.98$; Fig. 5A). Sixty percent (6/10) of *E. anna* matings experienced interruptions, which was not significantly different from the hybrid matings (61.5%, eight of 13; Fisher's exact test, $P = 1.0$; no data on *E. carunculatum* interruptions). The total duration of these interruptions was also not significantly different between *E. anna* or hybrid pairs ($t_{13.26} = -1.51$, $P = 0.15$; Fig. 5B). Although it has been suggested that Lepidoptera (Lorkovic 1958) and *Ischnura* (Córdoba-Aguilar and Cordero-Rivera 2008) use copulatory morphology or stimulation to identify conspecifics, our results indicate that this type of tactile discrimination during copula does not occur in *Enallagma*.

Similar proportions of *E. anna* (94.3%; 33 of 35) and hybrid females (76.9%, 10 of 13) oviposited after mating with *E. anna* males (Fisher's exact test, $P = 0.81$). Two *E. anna* females mated with hybrid males, but neither laid any eggs. In contrast, two *E. carunculatum* females mated with hybrid males and both oviposited. Two of the three hybrid females that mated with hybrid males also oviposited. Dissections of females that failed to oviposit confirmed that they had been inseminated and possessed mature eggs, and dissections of hybrid males in these matings confirmed that hybrid males produce motile sperm. *Enallagma anna*, *E. carunculatum*, and hybrid parings also produced comparable numbers of eggs ($F_{2,80} = 0.79$, $P = 0.46$; Fig. 5C). Although there appears to be a trend toward smaller clutches or complete failure to oviposit in females mated to hybrids, small samples prevent us from drawing strong conclusions about whether tactile incompatibilities might contribute to postcopulatory isolating mechanisms.

Laboratory generation 2 consisted solely of *E. anna* and advanced generation hybrid clutches, because in generation 1, *E. carunculatum* adults emerged earliest and few were available for crosses with *E. anna* or hybrids. In generation 2, *E. anna* and hybrid clutches had similar fertilization rates ($F_{1,17} = 0.51$, $P = 0.49$). In generation 1, *E. anna*, *E. carunculatum*, and hybrid clutches had similar proportions of hatched eggs (Kruskal–Wallis $\mathcal{X}_2^2 = 1.3385$, $P = 0.51$; Fig. 5C). In generation 2, *E. anna*, and hybrid clutches had similar proportions of hatched eggs ($t_{17.97} = 0.49404$, $P = 0.63$, Fig. S6). Oviposition date had a significant effect on hatch timing in generation 1 ($F_{1,41} = 49.1$, $P = 1.6 \times 10^{-8}$), but not in generation 2 ($F_{1,41} = 2.96$, $P = 0.11$). We therefore analyzed hatch timing separately for each generation. In generation 1, *E. carunculatum* larvae hatched earlier (15.4 ± 0.9 days, $n =$ 19 families) than *E. anna* (19.2 ± 0.7 days, $n = 17$ families) and hybrid larvae (20.0 ± 1.3 days, $n = 7$ families; analysis of covariance [ANCOVA] with oviposition date as covariate, $F_{2,39} = 10.8$, $P = 2 \times 10^{-4}$). In generation 2, *E. anna* and hybrid hatch rates did not differ significantly ($t_{11.92} = -1.22$, $P = 0.25$; Fig. 5D). If *E. carunculatum* larvae develop at a faster rate in the wild as they did in the laboratory, this could contribute to RI via seasonal temporal isolation, in which early emerging *E. carunculatum* adults are less likely to encounter, and thus potentially interbreed with, *E. anna* adults. Detecting and measuring this potential temporal barrier will require regular sampling throughout the breeding season.

An anomalous water quality problem at the Aquatic Research Facility where larvae were housed caused substantial larval mortality of generation 2, so we analyzed larval development timing for generation 1 only (Fig. 5F). An ANCOVA with oviposition

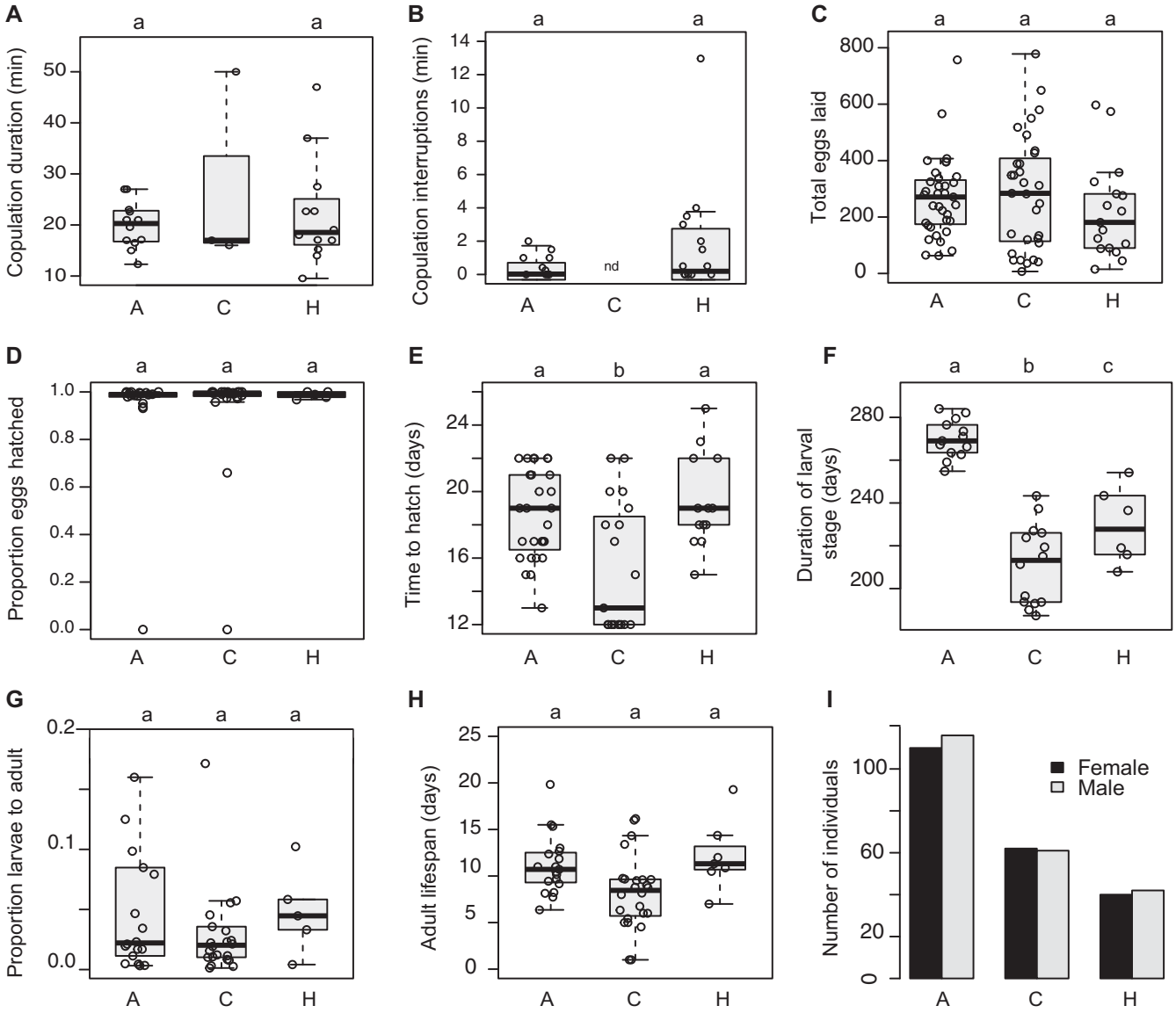

Figure 5. Sequentially acting mechanisms of postmating reproductive isolation. (A) Copulation duration. (B) Length of copulation interruptions. (C) Fecundity (field-caught and laboratory-reared data). (D) Proportion-hatched eggs per clutch. (E) Embryonic development timing. (F) Larval maturation timing. (G) Larval survivorship. (H) Adult life span. (I) Adult sex ratios. In panels (A) and (B), each point represents one male–female pair. "nd" denotes no data. In panels (C–G), each point represents one clutch. Within each panel, letters indicate homogeneous groups assigned at the statistical cutoff $\alpha = 0.05$. Box plots show the interquartile range. The line within the box shows the median and whiskers extend to the most extreme observation within ±1.5 times the interquartile range. Each open circle represents one mating pair (A, B), one clutch (C–E, G), or the clutch mean (F, H).

date as a covariate and Tukey's post hoc tests indicated that hybrids and parental species spent significantly different lengths of time in the larval stage ($F_{2,29} = 97.3$, $P < 1.4 \times 10^{-13}$). *Enallagma carunculatum* ($n = 13$ families) larvae reached adulthood at an average of 58.6 ± 2.5 days earlier than *E. anna* ($n = 14$ families; $P < 1 \times 10^{-5}$) and 18.2 ± 7.3 days earlier than hybrids ($n = 6$ families; $P = 0.056$). Hybrid larvae also developed significantly faster than *E. anna* ($P = 3 \times 10^{-5}$). Although *E. carunculatum* larvae developed faster than *E. anna* and hybrid larvae in the laboratory, mean adult abdomen length was similar among all three groups for both males ($F_{2,19} = 0.334$, $P = 0.72$) and females ($F_{2,21} = 3.30$, $P = 0.57$; Fig. S5). These results suggest that hybrid development was not affected by intrinsic genetic incompatibilities.

Larval survivorship in the laboratory was similar for both parental species' and hybrid clutches (Kruskal–Wallis $\mathcal{X}^2_2 = 4.4$, $P = 0.1$; Fig. 5G). Of those individuals that reached adulthood, adult life spans under laboratory conditions did not differ

significantly (ANCOVA with emergence date as covariate, $F_{2, 48} = 1.35$, $P = 0.29$; Fig. 5H). Finally, adult sex ratios were not significantly different from the expected 1:1 ratio for any group (Fig. 5I), which shows that among pure species and hybrids, both sexes had similar viability. The combination of our postmating isolation results demonstrate that neither strong intrinsic nor extrinsic (e.g., ecological selection against hybrids in the field) postzygotic barriers exist between *E. anna* and *E. carunculatum*.

Because heterospecific and hybrid matings were rare, we pooled the data obtained from reciprocal F_1s and advanced generation hybrid individuals to calculate postzygotic isolation. Although pooling these data could weaken the estimate of F_1 fitness loss, our field collection, behavior, and rearing data together suggest that the strength of intrinsic postzygotic RI between *E. anna* and *E. carunculatum* is minor compared to the strength of RI caused by intermediate reproductive structure morphologies.

DIVERGENT REPRODUCTIVE STRUCTURES CAUSE REPRODUCTIVE ISOLATION EARLY DURING SPECIATION

Figure 6 shows the cumulative strength of RI barriers measured for each reciprocal cross. Premating mechanical and tactile incompatibilities form the most substantial barriers to gene flow between *E. anna* and *E. carunculatum*, whereas later-acting barriers contribute little to total RI. Our results thus unequivocally demonstrate the potential of divergent mating structures to cause RI in the early stages of speciation via mechanical and tactile mechanisms. These incompatibilities also appear to provide particularly strong barriers to gene flow, as they act as both a premating barrier between pure species and also as a postzygotic barrier that reduces hybrid male mating success. Such incompatibilities represent a potent barrier to gene flow and may be a common characteristic of traits that are under sexual selection within species (Stratton and Uetz 1986; Naisbit et al. 2001; Höbel et al. 2003; Svedin et al. 2008; Van Der Sluijs et al. 2008).

Our results also show that premating barriers appear to have evolved first in *Enallagma*. Because *E. anna* × *E. carunculatum* hybrids appear to survive as well as parental species and suffer no intrinsic fertility deficits, the primary factor likely to affect their fitness is with whom they can mate. We observed that *E. anna* females often refuse to mate with conspecific males, indicating strong intraspecific discrimination. If the male cerci are under sexual selection similar to non-intromittent mating structures in other taxa (reviewed in Simmons 2014), and if females rely on the same tactile cues for both intraspecific mate choice and species discrimination, then female discrimination among conspecific males could extend to discrimination of heterospecific males. Prezygotic RI has been shown to evolve rapidly under laboratory settings due to assortative mating, independent of local adaptation (Castillo et al. 2015), which supports the plausibility of rapid evolution of RI driven by sexual selection in the wild. Female discrimination against males with intermediate cerci also provides an opportunity for reinforcement to strengthen premating isolation between *E. anna* and *E. carunculatum*— a potential example of sexual selection rather than natural selection driving reinforcement (Naisbit et al. 2001). Reinforcement could result in shifting or narrowing of female preferences (Ritchie 1996) or an increase in female discrimination in regions of sympatry (Noor 1999), two ideas that deserve further study in these species. Alternatively, evolution of cercus morphology may be driven by sexual

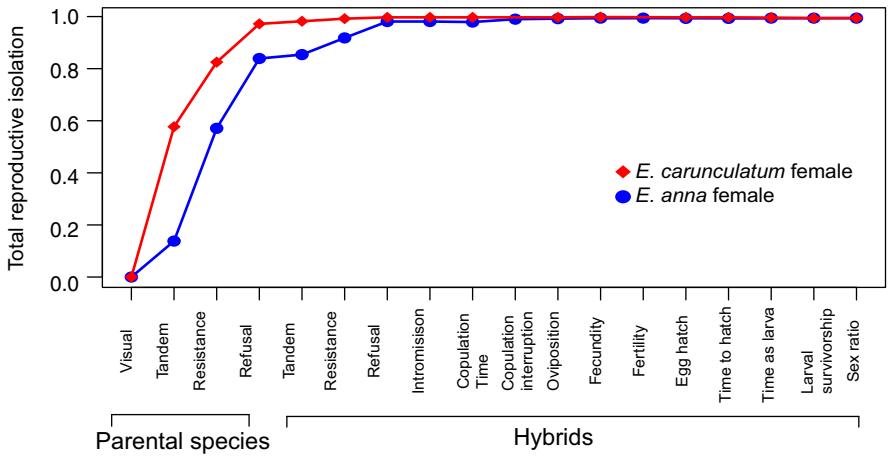

Figure 6. Sequential strength of reproductive isolating barriers, beginning with male–female encounter, and proceeding through the reproductive sequence and life history. Estimates of the strength of the first four barriers were obtained from conspecific and heterospecific crosses only, and estimates of the remaining barriers also include crosses involving hybrid individuals. Estimates for the values of the strength of two barriers from the *E. carunculatum* female × hybrid male cross (copulation interruption duration and fertility) are represented by the best-fit line at these barriers.

conflict over mating rate, in which selection favors females that are less easily grasped by males (Fincke et al. 2007).

Many researchers have dismissed genital mechanical incompatibilities as having an important role in RI and speciation (reviewed in Shapiro and Porter 1989; Eberhard 2010), primarily because of the small number of convincing cases that show strict support for it. We might be better equipped to investigate the reproductive consequences of the widespread pattern of rapid, divergent evolution of male genitalia if we broaden our scope to include explicitly tactile mechanisms. This may require dropping the genital "lock-and-key" imagery—which often evokes an "all or nothing" scenario in causing RI—in favor of a framework that allows for more variation, similar to our understanding of auditory, visual, and chemical communication signals. Indeed, our data show that mechanical isolation can be strong yet incomplete, and that tactile isolation can form a strong subsequent mating barrier. A full understanding of the contribution of mechanical incompatibilities in RI will require detailed morphological study to understand how male and female structures interact (e.g., Willkommen et al. 2015) and which features cause morphological mismatch. A deeper understanding of tactile RI mechanisms will require detailed studies of sensory mechanisms and the neurobiological basis of female reproductive decisions, all of which are admittedly challenging to investigate. Where females discriminate against heterospecific reproductive structures (e.g., Bath et al. 2012), the female nervous system poses a potentially more complex spectrum of incompatibilities compared to genitalia. Taxa such as damselflies or stick insects (Myers et al. 2016) provide ideal systems to begin to tease apart mechanical and tactile contributions to RI. Neural circuits that integrate olfactory and auditory cues with internal physiological processes to influence female mating decisions are being mapped in *Drosophila* (Bussell et al. 2014; Feng et al. 2014; Zhou et al. 2014), paving the way for similar mechanistic understanding of sensory modalities in emerging model systems. Although odonates have a unique mode of mating that presents multiple opportunities for both mechanical and tactile mismatch, our results highlight the potential contribution of tactile signals involving the genitalia to RI among internally fertilizing animals.

AUTHOR CONTRIBUTIONS

AAB, OMF, and JPM conceived the project; AAB and JPM designed the experiments; AAB performed the experiments and analyzed the data; AAB, MAM, and JPM contributed tools and reagents; and AAB and JPM wrote the paper with input from the other authors.

DATA ARCHIVING

The doi for our data is https://doi.org/10.5061/dryad.p6030.

LITERATURE CITED

Abramoff, M. D., P. J. Magalhaes, and S. J. Ram. 2004. Image processing with ImageJ. Biophoton. Int. 11:36–42.

Adams, D. C., and E. Otarola-Castillo. 2013. Geomorph: an R package for the collection and analysis of geometric morphometric shape data. Methods Ecol. Evol. 4:393–399.

Anderson, C. M., and R. B. Langerhans. 2015. Origins of female genital diversity: predation risk and lock-and-key explain rapid divergence during an adaptive radiation. Evolution 69:2452–2467.

Arnqvist, G. 1989. Sexual selection in a water strider: the function, mechanism of selection and heritability of a male grasping apparatus. Oikos 56:344–350.

Arnqvist, G., and L. Rowe. 2005. Sexual conflict. Princeton Univ. Press, Princeton, NJ.

Bath, E., N. Tatarnic, and R. Bonduriansky. 2012. Asymmetric reproductive isolation and interference in neriid flies: the roles of genital morphology and behaviour. Anim. Behav. 84:1331–1339.

Battin, T. J. 1993. The odonate mating system, communication, and sexual selection: a review. Bull. Zool. 60:353–360.

Bergsten, J., A. Töyrä, and A. N. Nilsson. 2001. Intraspecific variation and intersexual correlation in secondary sexual characters of three diving beetles (Coleoptera: Dytiscidae). Biol. J. Linn. Soc. 73:221–232.

Bertin, A., and D. Fairbairn. 2005. One tool, many uses: precopulatory sexual selection on genital morphology in Aquarius remigis. J. Evol. Biol. 18:949–961.

Bick, G. H., and J. C. Bick. 1981. Heterospecific pairing among Odonata. Odonatologica 10:259–270.

Bourret, A., M. A. McPeek, and J. Turgeon. 2012. Regional divergence and mosaic spatial distribution of two closely related damselfly species (*Enallagma hageni* and *Enallagma ebrium*). J. Evol. Biol. 25:196–209.

Brennan, P. L. 2016. Studying genital coevolution to understand intromittent organ morphology. Integr. Comp. Biol. 56:669–681.

Bussell, J. J., N. Yapici, S. X. Zhang, B. J. Dickson, and L. B. Vosshall. 2014. Abdominal-B neurons control *Drosophila* virgin female receptivity. Curr. Biol. 24:1584–1595.

Butlin, R., A. Debelle, C. Kerth, R. R. Snook, L. W. Beukeboom, C. R. Castillo, W. Diao, M. E. Maan, S. Paolucci, and F. J. Weissing. 2012. What do we need to know about speciation? Trends Ecol. Evol. 27:27–39.

Callahan, M. S., and M. A. McPeek. 2016. Multi-locus phylogeny and divergence time estimates of *Enallagma* damselflies (Odonata: Coenagrionidae). Mol. Phylogenet. Evol. 94:182–195.

Castillo, D. M., M. K. Burger, C. M. Lively, and L. F. Delph. 2015. Experimental evolution: assortative mating and sexual selection, independent of local adaptation, lead to reproductive isolation in the nematode *Caenorhabditis remanei*. Evolution 69:3141–3155.

Catling, P. M. 2001. Morphological evidence for the hybrid *Enallagma ebrium* x *hageni* (Zygoptera: Coenagrionidae) from Ontario. Proc. Entomol. Soc. Ontario 132:99–101.

Corbet, P. S. 1999. Dragonflies: behaviour and ecology of Odonata. Cornell Univ. Press, Ithaca, NY.

Córdoba-Aguilar, A., and A. Cordero-Rivera. 2008. Cryptic female choice and sexual conflict. Pp. 189–202 *in* A. Córdoba-Aguilar, ed. Dragonflies and damselflies: model organisms for ecological and evolutionary research. Oxford Univ. Press, New York, NY.

Coyne, J. A. 1993. The genetics of an isolating mechanism between two sibling species of *Drosophila*. Evolution 47:778–788.

Coyne, J. A., and H. A. Orr. 1997. "Patterns of speciation in *Drosophila*" revisited. Evolution 51:195–303.

———. 2004. Speciation. Sinauer Associates, Sunderland, MA.

Danielsson, I., and C. Askenmo. 1999. Male genital traits and mating interval affect male fertilization success in the water strider *Gerris lacustris*. Behav. Ecol. Sociobiol. 46:149–156.

de Wilde, J. 1964. Reproduction. Pp. 9–58 *in* M. Rockstein, ed. The physiology of Insecta. Academic Press, New York, NY.

Donnelly, N. T. 2008. A hybrid complex in *Enallagma*. Argia 20:10–11.

Dufour, L. 1844. Anatomie générale des diptéres. Ann. Sci. Nat. 1:244–264.

Eberhard, W. G. 1985. Sexual selection and animal genitalia. Harvard Univ. Press, Cambridge, MA.

———. 1992. Species isolation, genital mechanics, and the evolution of species-specific genitalia in three species of *Macrodactylus* Beetles (Coleoptera, Scarabeidae, Melolonthinae). Evolution 46:1774–1783.

———. 2001. Species-specific genitalic copulatory courtship in Sepsid flies (Diptera, Sepsidae, Microsepsis) and theories of genitalic evolution. Evolution 55:93–102.

———. 2010. Evolution of genitalia: theories, evidence, and new directions. Genetica 138:5–18.

Federley, H. 1932. Die bedeutung der kreuzung für die evolution. Jenische Zeitschrift für Naturwissenschaft 67:364–386.

Feng, K., M. T. Palfreyman, M. Häsemeyer, A. Talsma, and B. J. Dickson. 2014. Ascending SAG neurons control sexual receptivity of *Drosophila* females. Neuron 83:135–148.

Fincke, O. M. 2015. Trade-offs in female signal apparency to males offer alternative anti-harassment strategies for colour polymorphic females. J. Evol. Biol. 28:931–943.

Fincke, O. M., A. Fargevieille, and T. D. Schultz. 2007. Lack of innate preference for morph and species identity in mate-searching *Enallagma* damselflies. Behav. Ecol. Sociobiol. 61:1121–1131.

Forbes, M. R. 1991. Female morphs of the damselfly *Enallagma boreale* Selys (Odonata: Coenagrionidae): a benefit for androchromatypes. Canad. J. Zool. 69:1969–1970.

Frazee, S. R., and J. P. Masly. 2015. Multiple sexual selection pressures drive the rapid evolution of complex morphology in a male secondary genital structure. Ecol. Evol. 5:4437–4450.

Grant, V. 1992. Floral isolation between orithophilous and spingophilous species of *Ipomospsis* and *Aquilegia*. Proc. Natl. Acad. Sci. 89:11828–11831.

Hilton, D. F. J. 1983. Mating isolation in two species of *Nehalennia*. Odonatologica 12:375–379.

Höbel, G., H. Carl Gerhardt, and M. Noor. 2003. Reproductive character displacement in the acoustic communication system of green tree frogs (*Hyla cinerea*). Evolution 57:894–904.

House, C. M., and L. W. Simmons. 2003. Genital morphology and fertilization success in the dung beetle *Onthophagus taurus*: an example of sexually selected male genitalia. Proc. R. Soc. Lond. B Biol. Sci. 270:447–455.

Husband, B. C., and H. A. Sabara. 2004. Reproductive isolation between autotetraploids and their diploid progenitors in fireweed, *Chamerion angustifolium* (Onagraceae). New Phytol. 161:703–713.

Johansson, B. G., and T. M. Jones. 2007. The role of chemical communication in mate choice. Biol. Rev. 82:265–289.

Jordan, K. 1896. On mechanical selection and other problems. Novit. Zool. 3:426–525.

Kamimura, Y., and H. Mitsumoto. 2012. Lock-and-key structural isolation between sibling *Drosophila* species. Entomol. Sci. 15:197–201.

Kay, K. M. 2006. Reproductive isolation between two closely related hummingbird pollinated neotropical gingers. Evolution 60:538–552.

Kennedy, C. H. 1919. A study of the phylogeny of the Zygoptera from evidence given from the genitalia. Cornell University, Ithaca, NY.

Krieger, F., and E. Krieger-Loibl. 1958. Beiträge zum Verhalten von *Ischnura elegans* und *Ischnura pumilio* (Odonata) 1. Z. Tierpsychol. 15:82–93.

LeVasseur-Viens, H., M. Polak, and A. J. Moehring. 2015. No evidence for external genital morphology affecting cryptic female choice and reproductive isolation in *Drosophila*. Evolution 69:1797–1807.

Loibl, E. 1958. Zur Ethologie und Biologie der deutschen Lestiden (Odonata) 1. Z. Tierpsychol. 15:54–81.

Lorkovic, Z. 1953. L'accouplement artificiel chez les Lepidoptéres et son application dans les recherches sur la fonction de l'appareil génital des insectes. Physiol. Comp. Oecol. 3:313–320.

———. 1958. Some peculiarities of spatially and sexually restricted gene exchange in the *Erebia tyndarus* group. Cold Spring Harb. Symp. Quant. Biol. 23:319–325.

Masly, J. P. 2012. 170 Years of "Lock-and-Key": genital morphology and reproductive isolation. Int. J. Evol. Biol. 2012:1–10.

McMillan, W. O., C. Jiggins, and J. Mallet. 1997. What initiates speciation in passion-vine butterflies? Proc. Natl. Acad. Sci. USA 94:8628–8633.

McPeek, M. A., L. Shen, J. Z. Torrey, and H. Farid. 2008. The tempo and mode of three-dimensional morphological evolution in male reproductive structures. Am. Nat. 171:E158–E178.

McPeek, M. A., L. Shen, and H. Farid. 2009. The correlated evolution of three-dimensional reproductive structures between male and female damselflies. Evolution 63:73–83.

Mendelson, T. C., and G. Wallis. 2003. Sexual isolation evolves faster than hybrid inviability in a diverse and sexually dimorphic genus of fish (Percidae: *Etheostoma*). Evolution 57:317–327.

Miller, K. B., and M. A. Ivie. 1995. *Enallagma optimolocus*: a new species of damselfly from Montana (Odonata: Coenagrionidae). Proc. Entomol. Soc. Wash. 97:833–838.

Miller, M. N., and O. M. Fincke. 1999. Cues for mate recognition and the effect of prior experience on mate recognition in *Enallagma* damselflies. J. Insect Behav. 12:801–814.

———. 2004. Mistakes in sexual recognition among sympatric Zygoptera vary with time of day and color morphism (Odonata: Coenagrionidae). Int. J. Odonatol. 7:471–491.

Myers, S. S., T. R. Buckley, and G. I. Holwell. 2016. Male genital claspers influence female mate acceptance in the stick in sect *Clitarchus hookeri*. Behav. Ecol. Sociobiol. 70:1547–1556.

Naisbit, R. E., C. D. Jiggins, and J. Mallet. 2001. Disruptive sexual selection against hybrids contributes to speciation between *Heliconius cydno* and *Heliconius melpomene*. Proc. R. Soc. Lond. B Biol. Sci. 268:1849–1854.

Noor, M. F. 1999. Reinforcement and other consequences of sympatry. Heredity 83:503–508.

Otronen, M. 1998. Male asymmetry and postcopulatory sexual selection in the fly *Dryomyza anilis*. Behav. Ecol. Sociobiol. 42:185–191.

Panhuis, T. M., R. Butlin, M. Zuk, and T. Tregenza. 2001. Sexual selection and speciation. Trends Ecol. Evol. 16:364–371.

Paulson, D. R. 1974. Reproductive isolation in damselflies. Syst. Zool. 23:40–49.

Poelstra, J. W., N. Vijay, C. M. Bossu, H. Lantz, B. Ryll, I. Müller, V. Baglione, P. Unneberg, M. Wikelski, and M. G. Grabherr. 2014. The genomic landscape underlying phenotypic integrity in the face of gene flow in crows. Science 344:1410–1414.

Presgraves, D. C. 2002. Patterns of postzygotic isolation in Lepidoptera. Evolution 56:1168–1183.

Price, C. S., C. H. Kim, C. J. Gronlund, and J. A. Coyne. 2001. Cryptic reproductive isolation in the *Drosophila simulans* species complex. Evolution 55:81–92.

Price, T. D., and M. M. Bouvier. 2002. The evolution of F1 postzygotic incompatibilities in birds. Evolution 56:2083–2089.

R Core Team. 2015. R: a language and environment for statistical computing. R Foundation for Statistical Computing, Vienna, Austria.

Ramsey, J., H. D. J. Bradshaw, and D. W. Schemske. 2003. Components of reproductive isolation between the Monkey flowers *Mimulus lewisii* and *M. cardinalis* (Phrymaceae). Evolution 57:1520–1534.

Richards, O. W., and G. C. Robson. 1926. The species problem and evolution. Nature 117:345–347.

Ritchie, M. G. 1996. The shape of female mating preferences. Proc. Natl. Acad. Sci. USA 93:14628–14631.

Robertson, H. M., and H. E. H. Paterson. 1982. Mate recognition and mechanical isolation in *Enallagma* damselflies (Odonata: Coenagrionidae). Evolution 36:243–250.

Rodriguez, V., D. M. Windsor, and W. G. Eberhard. 2004. Tortoise beetle genitalia and demonstrations of a sexually selected advantage for flagellum length in *Chelymorpha alternans* (Chrysomelidae, Cassidini, Stolaini). Pp. 739–748 in New developments in the biology of Chrysomelidae, P. Jolivet, J.A. Santiago-Blay, and M. Schmitt, eds. SPB Academic Publishing, The Hague.

Rohlf, F. J. 1999. Shape statistics: procrustes superimpositions and tangent spaces. J. Classification 16:197–223.

Russell, S. T. 2003. Evolution of intrinsic post-zygotic reproductive isolation in fish. Ann. Zool. Fennici 40:321–329.

Ryan, M. J., and W. Wilczynski. 1991. Evolution of intraspecific variation in the advertisement call of a cricket frog (*Acris crepitans*, Hylidae). Biol. J. Linn. Soc. 44:249–271.

Sánchez-Guillén, R. A., M. Wellenreuther, and A. Cordero Rivera. 2012. Strong asymmetry in the relative strengths of prezygotic and postzygotic barriers between two damselfly sister species. Evolution 66:690–707.

Sánchez-Guillén, R. A., A. Cordoba-Aguilar, A. Cordero Rivera, and M. Wellenreuther. 2014. Rapid evolution of prezygotic barriers in non-territorial damselflies. Biol. J. Linn. Soc. 113:485–496.

Schick, R. X. 1965. The crab spiders of California (Araneida, Thomisidae). Bull. Am. Mus. Nat. Hist. 129:1–180.

Shapiro, A. M., and A. H. Porter. 1989. The lock-and-key hypothesis: evolutionary and biosystematic interpretation of insect genitalia. Ann. Rev. Entomol. 34:321–345.

Shaw, K. L. 1996. Polygenic inheritance of a behavioral phenotype: interspecific genetics of song in the Hawaiian cricket genus *Laupala*. Evolution 51:256–266.

Shen, L., H. Farid, and M. A. McPeek. 2009. Modeling three-dimensional morphological structures using spherical harmonics. Evolution 63:1003–1016.

Siepielski, A. M., K.-L. Hung, E. E. B. Bein, and M. A. McPeek. 2010. Experimental evidence for neutral community dynamics governing an insect assemblage. Ecology 91:847–857.

Simmons, L. W. 2014. Sexual selection and genital evolution. Aust. Entomol. 53:1–17.

Simmons, L. W., C. M. House, J. Hunt, and F. Garcia-Gonzalez. 2009. Evolutionary response to sexual selection in male genital morphology. Curr. Biol. 19:1442–1446.

Singer, T. L. 1998. Roles of hydrocarbons in the recognition systems of insects. Am. Zool. 38:394–405.

Sobel, J. M., and Chen, G. F. 2014. Unification of methods for estimating the strength of reproductive isolation. Evolution 68:1511–1522.

Sota, T., and K. Kubota. 1998. Genital lock-and-key as a selective agent against hybridization. Evolution 52:1507–1513.

Standfuss, M. R. 1896. Handbuch der paläarktischen Gross-Schmetterlinge für Forscher und Sammler. Verlag von Gustav Fischer, Jena, Germany.

Stratton, G. E., and G. W. Uetz. 1986. The inheritance of courtship behavior and its role as a reproductive isolating mechanism in two species of *Schizocosa* wolf spiders (Araneae; Lycosidae). Evolution 40:129–141.

Svedin, N., C. Wiley, T. Veen, L. Gustafsson, and A. Qvarnström. 2008. Natural and sexual selection against hybrid flycatchers. Proc. R. Soc. Lond. B Biol. Sci. 275:735–744.

Tanabe, T., and T. Sota. 2008. Complex copulatory behavior and the proximate effect of genital and body size differences on mechanical reproductive isolation in the millipede genus *Parafontaria*. Am. Nat. 171:692–699.

Tennessen, K. J. 1975. Reproductive behavior and isolation of two sympatric Coenagrionid damselflies in Florida. Univ. of Florida, Gainesville, FL.

———. 1982. Review of reproductive isolating barriers in Odonata. Adv. Odonatol. 1:251–265.

Tregenza, T., and N. Wedell. 1997. Definitive evidence for cuticular pheromones in a cricket. Anim. Behav. 54:979–984.

Turelli, M., N. H. Barton, and J. A. Coyne. 2001. Theory and speciation. Trends Ecol. Evol. 16:330–343.

Turgeon, J., R. Stoks, R. A. Thum, J. A. Brown, and M. A. McPeek. 2005. Simultaneous quaternary radiations of three damselfly clades across the Holarctic. Am. Nat. 165:E78–E107.

Van Der Sluijs, I., T. J. Van Dooren, K. D. Hofker, J. J. van Alphen, R. B. Stelkens, and O. Seehausen. 2008. Female mating preference functions predict sexual selection against hybrids between sibling species of cichlid fish. Philos. Trans. R. Soc. Lond. B Biol. Sci. 363:2871–2877.

Wellenreuther, M., and R. A. Sánchez-Guillén. 2016. Nonadaptive radiation in damselflies. Evol. Appl. 9:103–118.

Westfall, M. J., and M. L. May. 2006. Damselflies of North America. Revised ed. Scientific Publishers, Inc., Gainesville, FL.

Wiley, D. F., N. Amenta, D. A. Alcantara, D. Ghosh, Y. J. Kil, E. Delson, W. Harcourt-Smith, F. J. Rohlf, K. St John, and B. Hamann. 2005. Evolutionary morphing. Pp. 431–438 *in* Proceedings of IEEE Visualization 2005 (VIS'05), Minneanapolis, MN.

Williams, T. H., and T. C. Mendelson. 2014. Quantifying reproductive barriers in a sympatric pair of darter species. Evol. Biol. 41:212–220.

Williamson, E. B. 1906. Copulation of odonata. Entomol. News 17:143–148.

Willkommen, J., J. Michels, and S. N. Gorb. 2015. Functional morphology of the male caudal appendages of the damselfly *Ischnura elegans* (Zygoptera: Coenagrionidae). Arthropod Struct. Dev. 44:289–300.

Wojcieszek, J. M., and L. W. Simmons. 2012. Evidence for stabilizing selection and slow divergent evolution of male genitalia in a millipede (*Antichiropus variabilis*). Evolution 66:1138–1153.

———. 2013. Divergence in genital morphology may contribute to mechanical reproductive isolation in a millipede. Ecol. Evol. 3:334–343.

Xu, M., and O. M. Fincke. 2011. Tests of the harassment-reduction function and frequency-dependent maintenance of a female-specific color polymorphism in a damselfly. Behav. Ecol. Sociobiol. 65:1215–1227.

Zhou, C., Y. Pan, C. C. Robinett, G. W. Meissner, and B. S. Baker. 2014. Central brain neurons expressing doublesex regulate female receptivity in *Drosophila*. Neuron 83:149–163.

Associate Editor: A. Sweigart
Handling Editor: M. Noor

Supporting Information

Additional Supporting Information may be found in the online version of this article at the publisher's website:

Figure S1. Overview of spherical harmonic (SPHARM) analysis of male cercus shape.
Figure S2. Female geometric morphometric landmarks.
Figure S3. PCA results of replicate 3-D geometric morphometric analysis of female mesostigmal plate shape.
Figure S4. Presence/absence of female resistance behaviors during mating observations with lab-reared damselflies.
Figure S5. Adult *Enallagma* abdomen length measurements.
Figure S6. Proportion of hatched eggs in lab generation 2.